JACS
JOURNAL OF THE AMERICAN CHEMICAL SOCIETY
Article
pubs.acs.org/JACS

Relative Unidirectional Translation in an Artificial Molecular Assembly Fueled by Light

Hao Li,[†] Chuyang Cheng,[†] Paul R. McGonigal,[†] Albert C. Fahrenbach,[†,∥] Marco Frasconi,[†] Wei-Guang Liu,[⊥] Zhixue Zhu,[†] Yanli Zhao,[#,○] Chenfeng Ke,[†] Juying Lei,[†] Ryan M. Young,[†,‡] Scott M. Dyar,[†] Dick T. Co,[†,‡] Ying-Wei Yang,[†,∥] Youssry Y. Botros,[†,§,◆,¶] William A. Goddard, III,[⊥,+] Michael R. Wasielewski,[†,‡] R. Dean Astumian,[◇] and J. Fraser Stoddart*[,†]

[†]Department of Chemistry, [‡]Department of Chemistry and Argonne-Northwestern Solar Energy Research Center, and [§]Department of Materials Science and Engineering, Northwestern University, 2145 Sheridan Road, Evanston, Illinois 60208, United States

[∥]State Key Laboratory of Supramolecular Structure and Materials, College of Chemistry, Jilin University, 2699 Qianjin Street, Changchun 130012, PR China

[⊥]Materials and Process Simulation Center, California Institute of Technology, Pasadena, California 91125, United States

[#]Division of Chemistry and Biological Chemistry, School of Physical and Mathematical Sciences, Nanyang Technological University, 21 Nanyang Link, Singapore 637371

[○]School of Materials Science and Engineering, Nanyang Technological University, 50 Nanyang Avenue, Singapore 639798

[◆]National Center for Nano Technology Research, King Abdulaziz City for Science and Technology, P.O. Box 6086, Riyadh 11442, Kingdom of Saudi Arabia

[¶]Intel Labs, Building RNB-6-61, 2200 Mission College Boulevard, Santa Clara, California 95054, United States

[+]NanoCentury KAIST Institute and Graduate School of EEWS (WCU), Korea Advanced Institute of Science and Technology (KAIST), 373-1 Guseong Dong, Yuseong Gu, Daejeon 305-701, Republic of Korea

[◇]Department of Physics, The University of Maine, 5709 Bennett Hall, Orono, Maine 04469-5709, United States

Supporting Information

ABSTRACT: Motor molecules present in nature convert energy inputs, such as a chemical fuel or incident photons of light, into directed motion and force biochemical systems away from thermal equilibrium. The ability not only to control relative movements of components in molecules but also to drive their components preferentially in one direction relative to each other using versatile stimuli is one of the keys to future technological applications. Herein, we describe a wholly synthetic small-molecule system that, under the influence of chemical reagents, electrical potential, or visible light, undergoes unidirectional relative translational motion. Altering the redox state of a cyclobis(paraquat-*p*-phenylene) ring simultaneously (i) inverts the relative heights of kinetic barriers presented by the two termini—one a neutral 2-isopropylphenyl group and the other a positively charged 3,5-dimethylpyridinium unit—of a constitutionally asymmetric dumbbell, which can impair the threading/dethreading of a [2]pseudorotaxane, and (ii) controls the ring's affinity for a 1,5-dioxynaphthalene binding site located in the dumbbell's central core. The formation and subsequent dissociation of the [2]pseudorotaxane by passage of the ring over the neutral and positively charged termini of the dumbbell component in one, and only one, direction relatively defined has been demonstrated by (i) spectroscopic (^{1}H NMR and UV/vis) means and cyclic voltammetry as well as with (ii) DFT calculations and by (iii) comparison with control compounds in the shape of constitutionally symmetrical [2]pseudorotaxanes, one with two positively charged ends and the other with two neutral ends. The operation of the system relies solely on reversible, yet stable, noncovalent bonding interactions. Moreover, in the presence of a photosensitizer, visible-light energy is the only fuel source that is needed to drive the unidirectional molecular translation, making it feasible to repeat the operation numerous times without the buildup of byproducts.

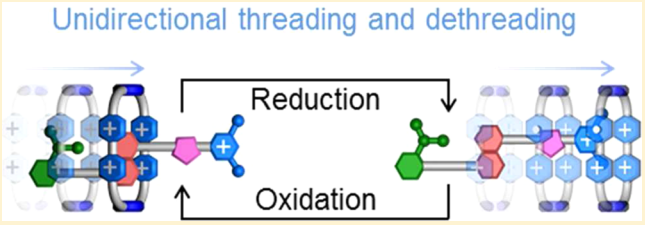

1. INTRODUCTION

One of the distinguishing features of living organisms is their proclivity to employ molecular machinery on a grand scale to power their metabolic processes.[1] Amidst all this machinery, motor molecules (MMs) are vital components that are required to drive biological systems away from thermal equilibrium and, in so doing, provide the impetus for all manner of important tasks, such as (i) ATP synthesis,[2] (ii) the transport of cellular cargo,[3] (iii) muscle contraction,[4] (iv) cellular locomotion,[5] and (v) the

Received: September 11, 2013
Published: October 30, 2013

dx.doi.org/10.1021/ja4094204 | J. Am. Chem. Soc. 2013, 135, 18609−18620

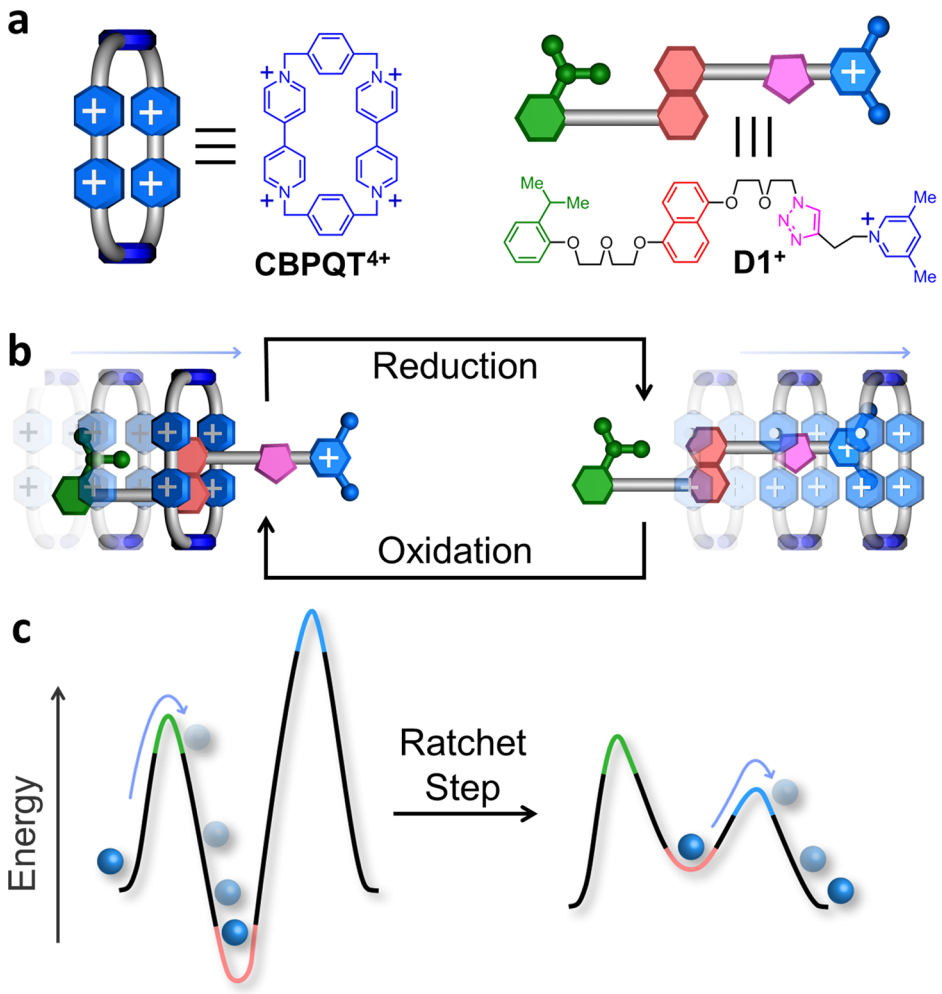

Figure 1. Graphical representation of a [2]pseudorotaxane pump with structural formulas and simplified potential energy diagrams of a flashing ratchet. (a) Structural formulas of the **CBPQT**$^{4+}$ ring and asymmetric dumbbell **D1**$^{+}$. Charges are balanced by hexafluorophosphate (PF_6^-) counterions, which are omitted for the sake of clarity. (b) Graphical representation of the operation of [2]pseudorotaxane **D1**$^{+}$⊂**CBPQT**$^{4+}$ in which the ring passes over a sterically bulky group (green) to reach an electron-rich binding site (red) under oxidative conditions before dethreading by passing over the positively charged end group (blue) when reduced. (c) A Brownian particle (blue sphere) under the influence of a potential energy surface moves to the lowest energy state (red trough) by passing over the lowest kinetic energy barrier (green peak). Simultaneously raising the potential energy well (red trough) so that it is no longer the minimum-energy state and reversing the relative heights of the energy barriers (green and blue peaks) causes the particle to continue. Flip-flopping between the two oxidized and reduced states (b) of pseudorotaxane **D1**$^{+}$⊂**CBPQT**$^{4+}$, with potential energy surfaces that qualitatively resemble those shown in panel c, creates directional and repetitive motion of the ring relative to the dumbbell.

active transport of sugars,[6] protons,[7] or other ions[8] across membranes. All of these processes occur on the nanoscale and are dominated by nonstop Brownian motion[9] caused by random collisions between molecules. Rather than attempting to overcome this directionless energy, which is essentially thermal noise, nature's MMs employ stochastic ratchet mechanisms[10] to convert this noise into useful work. Such "Brownian ratchets" create a net flux of particles in one direction by linking the oscillation between asymmetric potential energy surfaces—raising and lowering activation barriers and energy wells (e.g., Figure 1)—to the depletion of an external energy source. In this manner, the consumption of fuel (e.g., the hydrolysis of ATP or the dissipation of absorbed photons of light as heat) provides the means necessary to overcome the limitations imposed by the principle of microscopic reversibility[11] and maintains a non-equilibrium state in which useful work is performed.

Chemists, who have drawn inspiration from the advanced function displayed by nature's motors, are currently engaged in designing and creating artificial MMs that harness ratchet mechanisms to generate directed molecular motion and push systems away from equilibrium.[12] Although some of the most sophisticated man-made systems to date have been assembled and controlled by the unique molecular recognition properties of DNA strands,[13] remarkable progress has also been made in the realm of wholly synthetic small-molecule motors. Rotary motors[14] have been developed that display controlled circumrotations of interlocked rings[15] in some cases or rotations around single[16] or double bonds[17] in others. Feringa's sterically crowded olefin rotors[17] are particularly noteworthy examples that have been optimized and exploited in order to perform tasks as diverse as the spinning of a microscale object on a surface[17b] or diverting the course of an asymmetric chemical reaction.[17d] Their versatility and utility are rooted in the elegance of their switching mechanisms that (i) are powered by the absorption of light energy and (ii) occur autonomously; that is, while the fuel is present, the MMs cycle continually and directionally without any additional intervention.

Net linear translation of the constituent parts of mechanically interlocked molecular shuttles,[18] pseudorotaxanes,[19] and molecular

dx.doi.org/10.1021/ja4094204 | J. Am. Chem. Soc. 2013, 135, 18609−18620

Scheme 1. Synthesis of Dumbbell D1·PF_6

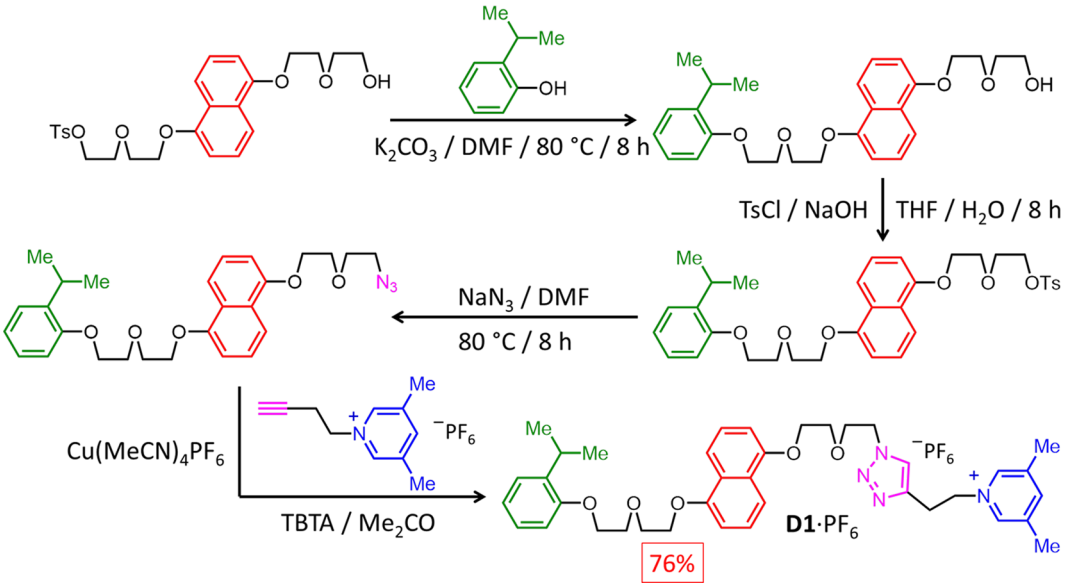

walkers[20] has also been achieved by exploiting ratchet mechanisms.[10] With the exception of information ratchets,[10e,18b−d] however, these systems require the stepwise input of more than one stimulus, often including the addition of chemical reagents.[18a,c,d,19,20] To achieve the requisite level of sophistication and functional attributes to allow useful work to be extracted from artificial linear ratchets, it is necessary to devise systems capable of operation under the application of a single versatile stimulus. Light and electricity[21] are particularly appealing stimuli for advanced devices because they benefit from ease of integration with existing technologies and, in principle, allow precise spatiotemporal control over switching.

Here, we report a wholly synthetic small-molecule system in the form of a [2]pseudorotaxane (Figure 1a) whose components undergo relative unidirectional translational motion (Figure 1b) driven by a single stimulus that simultaneously controls (Figure 1c) two kinetic barriers and one thermodynamic well. The [2]pseudorotaxane consists (Figure 1a) of a tetracationic π-accepting cyclobis(paraquat-*p*-phenylene)[22] (**CBPQT**$^{4+}$) ring and a constitutionally asymmetric dumbbell **D1**$^+$, which contains (Scheme 1) a π-donating 1,5-dioxynaphthalene (DNP) recognition site for the ring in the center of a polyether chain and is terminated at one end by a neutral 2-isopropylphenyl group and at the other end by a positively charged 3,5-dimethylpyridinium unit. We demonstrate, by employing (i) experimental comparisons with symmetrical control dumbbells[23] **D2**$^{2+}$ and **D3** bearing either two charged or two neutral ends (Scheme 2) and (ii) density functional theory (DFT) calculations, (iii) ^{1}H NMR spectroscopy, (iv) UV/vis spectroscopy, and (v) cyclic voltammetry (CV), that simply altering the redox state of the **CBPQT**$^{4+}$ ring is enough to oscillate its minimum-energy state and, at the same time, invert the relative heights of the kinetic barriers to dethreading over the termini, thereby favoring dethreading over the charged end group upon reduction. Oxidation of the **CBPQT**$^{2(\bullet+)}$ ring back to its tetracationic state elicits a contrary response on the part of the kinetic barriers presented to the ring, making it easier to thread over the neutral rather than the charged end. In other words, we show that the formation of the [2]pseudorotaxane, when the ring is in its most highly oxidized state, is followed, upon its partial reduction, by its dissociation, which occurs by passage onto, along, and off of the dumbbell in one direction relatively speaking (i.e., from left to right in relation to how the [2]pseudorotaxane is illustrated in Figure 1). Specifically, we demonstrate that reduction with Zn dust, followed by oxidation in air, can fuel this molecular-energy ratchet, as can the oscillating electrochemical potentials during cyclic

Scheme 2. Synthesis of Dumbbells D2·2PF_6 and D3 and Their Graphical Representations

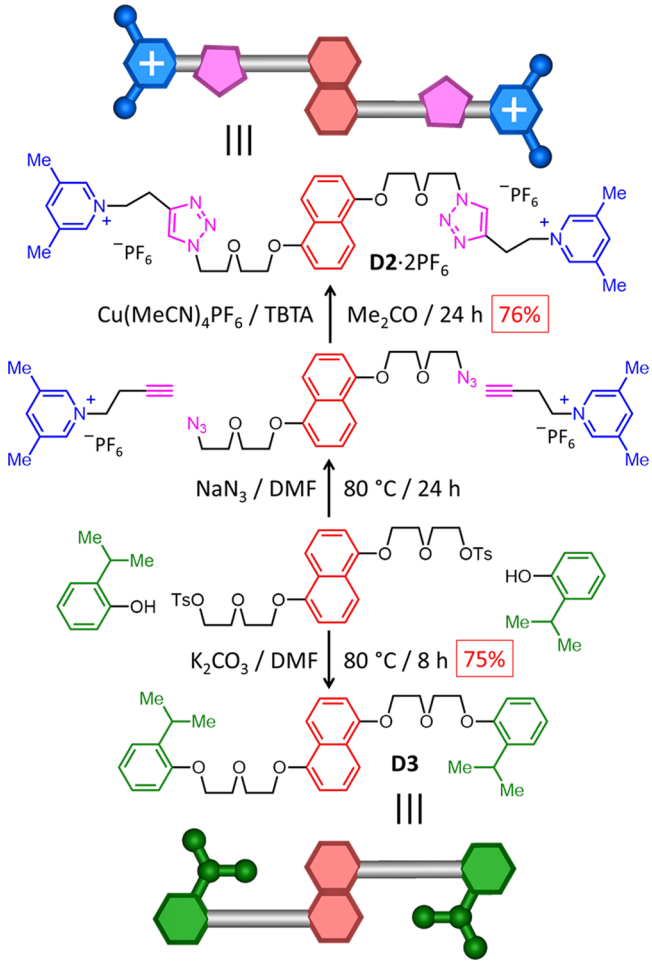

dx.doi.org/10.1021/ja4094204 | *J. Am. Chem. Soc.* 2013, 135, 18609−18620

voltammetry. Alternatively, we have shown that under appropriate experimental conditions, light can be supplied as the sole energy source to initiate a photoredox reaction that results in a continuous cycle of threading and dethreading of the [2]pseudorotaxane components in an asymmetric manner as illustrated in Figure 1b.

2. RESULTS AND DISCUSSION

2.1. Design Strategy. Tetracationic cyclophane **CBPQT**$^{4+}$ is well-established[22] as an electron-poor host that, on account of its propensity to form inclusion complexes with electron-rich aromatic guests, has been investigated[12e] extensively as a means of assembling mechanically interlocked molecules (MIMs) prior to manipulating the relative positions of their constituent parts. In recent times,[24,25] we have shown that the reduction of **CBPQT**$^{4+}$ to its radical states (**CBPQT**$^{(2+)(\bullet+)}$ and **CBPQT**$^{2(\bullet+)}$) dramatically alters its preference for guests. When contemplating the design of a [2]pseudorotaxane capable of unidirectional threading and dethreading, we recognized that the redox chemistry of this tetracationic cyclophane affords us the opportunity (Figure 1) to change simultaneously (i) the depth of a potential energy well associated with the stability of the donor−acceptor inclusion complex and (ii) the heights of a kinetic energy barrier arising from steric interactions between the positively charged ring and the neutral end of the dumbbell on the one hand and from the Coulombic repulsion between the positively charged ring and the positively charged end of the dumbbell on the other hand, thereby providing the fundamental basis for a flashing ratchet mechanism.[10c,12b,19a]

More specifically, we envisaged a system based upon the complexation of **CBPQT**$^{4+}$ with dumbbell **D1**$^{+}$, which incorporates (Figure 1) an electron-rich DNP unit in its midriff, flanked by a positively charged 3,5-dimethylpyridinium unit at one end and a neutral 2-isopropylphenyl group at the other end. Under oxidative conditions, association is driven by the π-electron donor−acceptor interactions between the DNP unit in the middle of **D1**$^{+}$ and the two BIPY^{2+} units present in **CBPQT**$^{4+}$. Before the ring reaches this minimum-energy coconformation, however, it must first traverse one of the two termini of the dumbbell. Transit of the tetracationic ring over the positively charged 3,5-dimethylpyridinium terminus is greatly disfavored on account of strong Coulombic repulsion.[26] The minimum-energy path to complex formation, therefore, involves passage over the sterically bulky yet neutral 2-isopropylphenyl group. Subsequent reduction of **CBPQT**$^{4+}$ to its partially neutralized, radical states (i) decreases the Coulombic repulsion between the 3,5-dimethylpyridinium unit and the ring quite considerably and (ii) attenuates the donor−acceptor interactions between the DNP unit and the ring,[27] thereby favoring the dissociation of the complex. As a result, the reduced ring slips off of the dumbbell into solution. It does so by passing over the terminal 3,5-dimethylpyridinium unit as opposed to retracing its path over the bulky 2-isopropylphenyl terminus because this latter pathway would involve surmounting the higher of the two free-energy barriers. Finally, reoxidation of the ring returns the system back to its initial fully charged state, with free **CBPQT**$^{4+}$ and **D1**$^{+}$ in solution ready to undergo another cycle.

We have introduced the term mechanostereoselectivity[25e] to describe relative translational or circumrotational motions that take place along one pathway in preference to another, in the context of MIMs or host−guest complexes. In essence, this type of selective motion is a kinetic phenomenon that occurs as a consequence of substantial differences between free-energy barriers. The relative mechanostereoselective motion that characterizes [2]pseudorotaxane **D1**$^{+}$⊂**CBPQT**$^{4+}$ arises from the constitutional asymmetry of the dumbbell and the relative heights of the kinetic energy barriers presented by the end groups, which are inverted upon changing the redox state of the ring. The implication is that the repetition of the redox cycle leads to recurring translations of the ring along the rod in one and only one direction from the 2-isopropylphenyl terminus to the 3,5-dimethylpyridinium terminus.

2.2. Syntheses of the Dumbbells. Asymmetrical dumbbell **D1**·PF_6 was obtained (Scheme 1) in four steps[28] starting from the monotosylate of 1,5-bis[2-(2-hydroxyethoxy)ethoxy]-naphthalene, and symmetrical dumbbells **D2**·2PF_6 and **D3** were synthesized (Scheme 2) from 1,5-bis[2-(2-hydroxyethoxy)ethoxy]-naphthalene, (**BHEEN**) the second (**D3**) from the ditosylate and the first (**D2**·2PF_6) from the bisazide prepared from the ditosylate.

2.3. Investigations under Oxidative Conditions. To shed light on the heights of the kinetic barriers that play such an important part in the redox cycling of **D1**$^{+}$⊂**CBPQT**$^{4+}$, which we expected to result in mechanostereochemical translation, we decided to investigate the behavior of symmetrical complexes, **D2**$^{2+}$⊂**CBPQT**$^{4+}$ and **D3**⊂**CBPQT**$^{4+}$ (Scheme 2) under both oxidative and reductive conditions. Model studies using rod **D2**$^{2+}$ allowed us to measure (Figure 2) the impedance to dethreading and threading resulting from Coulombic repulsion between the ring and the 3,5-dimethylpyridinium end, whereas investigations (Figure 3) using **D3** provided us with an understanding of the steric barrier presented to the ring by the 2-isopropylphenyl terminus.

Pyridinium-terminated pseudorotaxane **D2**$^{2+}$⊂**CBPQT**$^{4+}$ can be prepared by either slow slippage of the **CBPQT**$^{4+}$ ring onto dumbbell **D2**$^{2+}$ over a period of weeks or by introducing the 3,5-dimethylpyridinium end groups to a preformed pseudorotaxane precursor in a Cu-catalyzed azide−alkyne cycloaddition.[28] Dethreading of the ring is sufficiently slow on the laboratory time scale to allow the isolation of the inclusion complex by column chromatography; indeed, the ^{1}H NMR spectrum[28] of **D2**$^{2+}$⊂**CBPQT**$^{4+}$, recorded (Figure 2b) in CD_3CN, undergoes very little change during several weeks at ambient temperature. To gain a more quantitative understanding of the kinetic parameters controlling both the association to form **D2**$^{2+}$⊂**CBPQT**$^{4+}$ and its dissociation, we employed ^{1}H NMR spectroscopy to monitor the change in the composition of CD_3CN (0.5 mL) solutions that initially contained dumbbell **D2**·2PF_6 (1.2 mM) and excess of **CBPQT**·PF_6 (20−45 mM). We observed (Figure 2d) a concomitant decrease in the intensities of resonances associated with free dumbbell **D2**$^{2+}$ and an increase in those corresponding to 1:1 complex **D2**$^{2+}$⊂**CBPQT**$^{4+}$. After a period at ambient temperature ranging from 4 to 14 days and depending on the concentration of **CBPQT**$^{4+}$, no further change in the composition of the reaction mixture was observed, indicating that equilibrium had been reached. Using equation $K_a = [\mathbf{D2}^{2+}\subset\mathbf{CBPQT}^{4+}]/([\mathbf{D2}^{2+}][\mathbf{CBPQT}^{4+}])$, with the concentrations of each of the species determined by the relative integration of ^{1}H NMR signals, the binding constant (K_a) was measured to be 180 M^{-1} in CD_3CN at 298 K. The rate constant for the formation of **D2**$^{2+}$⊂**CBPQT**$^{4+}$ was calculated (Figure 2e) from a plot of pseudo-first-order rate constant k_{obs} versus the initial concentration of **CBPQT**$^{4+}$. From this plot, a rate of association $k_f = 2.0 \pm 0.2 \times 10^{-4}$ M^{-1} s^{-1} and in turn a rate of dissociation $k_b = 1.1 \pm 1.1 \times 10^{-6}$ s^{-1} could be deduced. Employing these kinetic data, we calculated that $k_{threading} = 1.0 \times 10^{-4}$ L mol^{-1} s^{-1}, $k_{dethreading} = 5.6 \times 10^{-7}$ s^{-1}, $\Delta G^{\ddagger}_{threading} = 22.9$ kcal mol^{-1}, and $\Delta G^{\ddagger}_{dethreading} = 25.9$ kcal mol^{-1}.

dx.doi.org/10.1021/ja4094204 | J. Am. Chem. Soc. 2013, 135, 18609−18620

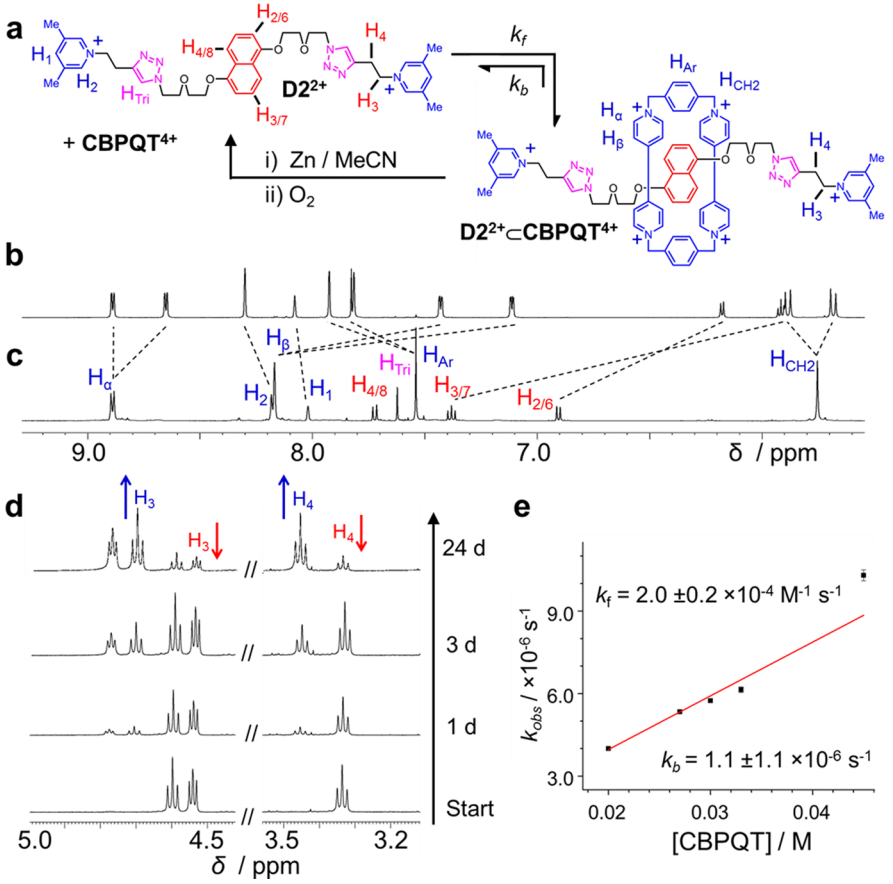

Figure 2. Determination of the kinetic parameters controlling the threading and dethreading of **CBPQT**$^{4+}$ over 3,5-dimethylpyridinium termini. (a) Equilibrium of **D2**·2PF$_6$ and **CBPQT**·PF$_6$ with pseudorotaxane **D2**·2PF$_6$⊂**CBPQT**·PF$_6$. Chemical reduction of **D2**·2PF$_6$⊂**CBPQT**·PF$_6$ with Zn, followed by oxidation in air, causes the ring to slip off the dumbbell; partial 600 MHz ^{1}H NMR spectra in CD_3CN (b) before and (c) after this chemical reduction and oxidation procedure show complete dissociation of the pseudorotaxane. (d) Mixtures of **D2**·2PF$_6$ and varying concentrations[28] of **CBPQT**·PF$_6$ were monitored by ^{1}H NMR spectra as the peaks corresponding to **D2**·2PF$_6$⊂**CBPQT**·PF$_6$ increased over time. (e) Apparent pseudo-first-order rate constant, k_{obs}, vs the concentration of **CBPQT**$^{4+}$, with the concentration of **D2**$^{2+}$ held constant, (i.e., $[\mathbf{D2}^{2+}]_0 = 1.2 \times 10^{-3}$ M). Solvent, CD_3CN; T = 298 K.

By contrast, it takes a relatively short amount of time, on the order of minutes, for unsymmetrical complex **D1**$^+$⊂**CBPQT**$^{4+}$ to reach equilibrium. If we assume, quite reasonably, that the energy barriers for the **CBPQT**$^{4+}$ ring to slip over the 3,5-dimethylpyridinium end of **D1**$^+$ are similar in magnitude to that determined using **D2**$^{2+}$, then the rapid rate of threading in this case has to be a result (Figure 3a) of the passage of the ring over the 2-isopropylphenyl end in a mechanostereoselective fashion. By measuring the rate of **D1**$^+$⊂**CBPQT**$^{4+}$ complex formation, therefore, we can determine the transition-state energy necessary to cross this steric barrier. We followed the change in intensity of an absorption peak at 520 nm in the UV/vis spectrum (Figure 3b, inset), which emerges as a consequence of charge transfer when the **CBPQT**$^{4+}$ ring encircles the DNP unit in the dumbbell in order to probe the concentration of the 1:1 (**D1**$^+$⊂**CBPQT**$^{4+}$) complex as a function of time. An increase in the absorbance at 520 nm in the time range of seconds was recorded (Figure 3b) for the formation of **D1**$^+$⊂**CBPQT**$^{4+}$, and this measurement was repeated at a variety of initial **CBPQT**·PF$_6$ concentrations to allow us to determine[28] the corresponding pseudo-first-order rate constants, k_{obs}. On the basis of these data, we deduced that $\Delta G^{\ddagger}_{threading}$ = 17.2 kcal mol^{-1} and $\Delta G^{\ddagger}_{dethreading}$ = 21.0 kcal mol^{-1}. Similar kinetics measurements were performed[28] to assess the energy barriers to threading and dethreading over the 2-isopropylphenyl termini of symmetrical dumbbell **D3**; values of $\Delta G^{\ddagger}_{threading}$ = 16.9 kcal mol^{-1} and $\Delta G^{\ddagger}_{dethreading}$ = 20.6 kcal mol^{-1} were determined, in close agreement with those measured for **D1**$^+$. When taken together with the barrier heights determined above for the 2,5-dimethylpyridinium ends of **D2**$^{2+}$, these $\Delta G^{\ddagger}$ values indicate that under oxidative conditions the rate at which the ring undergoes threading from the 2-isopropylphenyl end in dumbbell **D1**$^+$ is more than 4 orders of magnitude faster than that observed for threading from the 3,5-dimethylpyridinium end. Expressed another way, although it takes days for the charged ring to thread over the charged end of the asymmetric dumbbell, threading of the neutral end happens in minutes.

2.4. Investigations under Reductive Conditions. When Zn dust, a heterogeneous reducing agent that is capable[23d,g] of converting **CBPQT**$^{4+}$ to **CBPQT**$^{2(\bullet+)}$, was added to a CD_3CN solution of symmetrically charged dumbbell complex **D2**$^{2+}$⊂**CBPQT**$^{4+}$ under an inert atmosphere, the solution acquired a characteristic blue color indicative of radical formation. After[28] stirring for 2 min, the Zn dust was removed by filtration and the solution was exposed to air to regenerate the **CBPQT**$^{4+}$ ring. ^{1}H NMR spectroscopy revealed that the initial [2]pseudorotaxane **D2**$^{2+}$⊂**CBPQT**$^{4+}$ had reverted to a 1:1 mixture of free **D2**$^{2+}$ and **CBPQT**$^{4+}$, a result that is consistent with the rapid egress of the ring from the dumbbell upon reduction.

dx.doi.org/10.1021/ja4094204 | J. Am. Chem. Soc. 2013, 135, 18609−18620

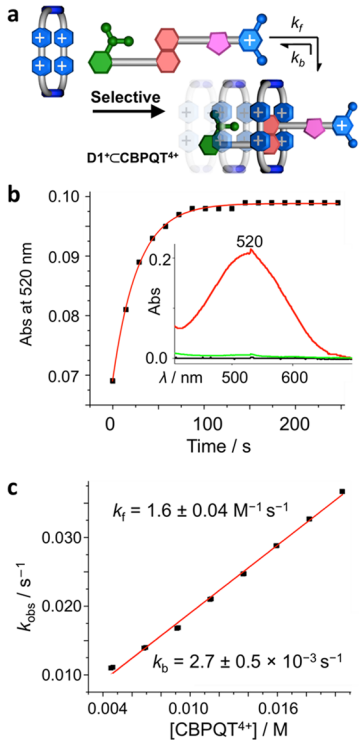

Figure 3. UV/vis absorption spectroscopy determination of the kinetic barrier to threading the 2-isopropylphenyl terminus through **CBPQT**$^{4+}$. (a) Graphical representation of the selective threading leading to the formation of inclusion complex **D1**$^{+}$⊂**CBPQT**$^{4+}$. (b) Kinetic trace for the formation of **D1**$^{+}$⊂**CBPQT**$^{4+}$ obtained by tracking the absorbance at 520 nm in the UV/vis absorption spectra recorded in MeCN at 298 K. The spectra were recorded every 14.5 s in a 1 mm cell-path-length cuvette. A single rate-limiting step is observed. $[\mathbf{D1}^{+}]_0 = 1.5 \times 10^{-3}$ M; $[\mathbf{CBPQT}^{4+}]_0 = 2.0 \times 10^{-2}$ M. (Inset) UV/vis absorption spectra of **CBPQT**$^{4+}$ (black trace), **D1**$^{+}$ (green trace), and **D1**$^{+}$⊂**CBPQT**$^{4+}$ (red trace) recorded in MeCN at 298 K. The formation of **D1**$^{+}$⊂**CBPQT**$^{4+}$ is characterized by a charge-transfer band centered close to 520 nm. (c) Plot of the apparent pseudo-first-order rate constant, k_{obs}, vs the concentration of **CBPQT**$^{4+}$, with the concentration of **D1**$^{+}$ held constant (i.e., $[\mathbf{D1}^{+}]_0 = 1.5 \times 10^{-3}$ M). Solvent, MeCN; T = 298 K.

So as to test our assumption that [2]pseudorotaxane **D1**$^{+}$⊂**CBPQT**$^{4+}$ undergoes reversible dissociation and association upon reduction and oxidation, respectively, a spectroelectrochemistry (SEC) experiment was conducted (Figure S8) using a mixture of dumbbell **D1**$^{+}$, **CBPQT**$^{4+}$, and methyl viologen (**V**$^{2+}$).[28] Upon application of a reductive voltage (−700 mV), the solution exhibited the characteristic maximum absorptions for radical-radical interactions, indicating the formation of [2]pseudorotaxane **V**$^{(\bullet+)}$⊂**CBPQT**$^{2(\bullet+)}$, as well as the dissociation of the **D1**$^{+}$⊂**CBPQT**$^{4+}$ complex. By subsequently decreasing the potential to 0 mV and exposing the solution to air, the absorbance resulting from the radical trimer diminished while the initial donor−acceptor charge-transfer band corresponding to **D1**⊂**CBPQT**$^{4+}$ reemerged, indicating that association and dissociation are reversible.

To evaluate the rates by which the reduced forms (**CBPQT**$^{2(\bullet+)}$/**CBPQT**$^{(\bullet+)(2+)}$) of **CBPQT**$^{4+}$ slip over the 2-isopropylphenyl and 3,5-dimethylpyridinium termini, we recorded (Figure 4) the cyclic voltammograms of all three [2]pseudorotaxanes, namely, **D1**$^{+}$⊂**CBPQT**$^{4+}$, **D2**$^{2+}$⊂**CBPQT**$^{4+}$, and **D3**⊂**CBPQT**$^{4+}$, in addition to performing density functional theory calculations[28] on the **D1**$^{+}$⊂**CBPQT**$^{4+}$ [2]pseudorotaxane. In the CV trace (Figure 4a) of **D3**⊂**CBPQT**$^{4+}$, the peaks observed at −0.31 and −0.40 V can be assigned to two one-electron reductions, that is, for **CBPQT**$^{4+}$/**CBPQT**$^{(2+)(\bullet+)}$ and **CBPQT**$^{(2+)(\bullet+)}$/**CBPQT**$^{2(\bullet+)}$, respectively. The stepwise reductions arise from the fact that upon the first one-electron reduction at −0.31 V of the BIPY^{2+} unit, which is not strongly engaged in donor−acceptor interactions, the dethreading of **D3**⊂**CBPQT**$^{(2+)(\bullet+)}$ is still opposed by the 2-isopropylphenyl termini. As a result, the monoradical tricationic **CBPQT**$^{(2+)(\bullet+)}$ ring resides on the rod for a substantial amount of time relative to the millisecond time scale of the CV scan, and its second BIPY^{2+} unit still interacts with the DNP portion of the dumbbell by virtue of donor−acceptor interactions. This second BIPY^{2+} unit, therefore, is relatively less π-electron deficient when compared to the first one and so undergoes reduction at the more negative peak potential of −0.40 V. Similar stepwise two-electron reductions were also observed[28] in the case of a [2]rotaxane (**R1**$^{4+}$) whose dissociation is prohibited by a fully fledged mechanical bond.

By contrast, in the case of **D2**$^{2+}$⊂**CBPQT**$^{4+}$, these two one-electron reductions are not observed as separate peaks: rather, a single two-electron reduction occurs (Figure 4b) at −0.33 V, indicating that once an electron is added to the first BIPY^{2+} unit, which is not strongly engaged in π-electron donor−acceptor interactions,[29] the 1:1 **D2**$^{2+}$⊂**CBPQT**$^{(2+)(\bullet+)}$ complex so formed undergoes rapid dissociation on the time scale of the CV

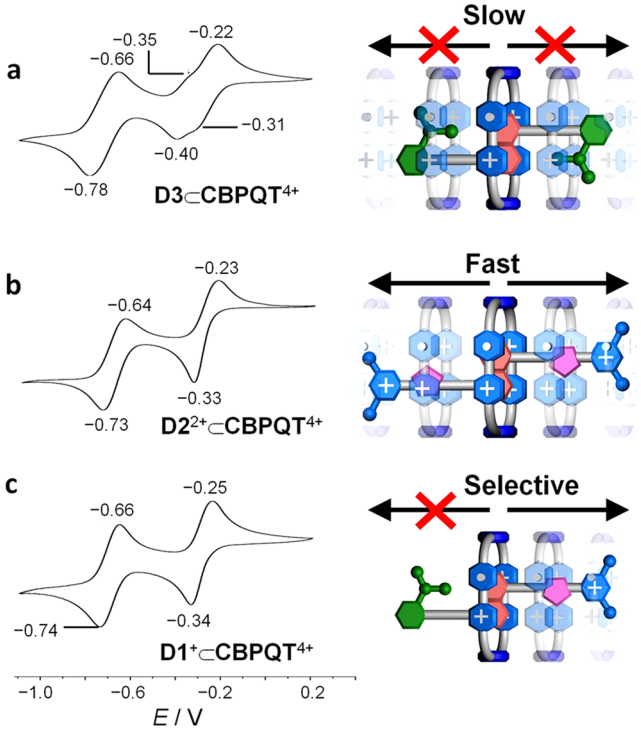

Figure 4. Reductive cyclic voltammograms (second scans, argon-purged MeCN, 0.1 M Bu_4NPF_6, 200 mV s^{-1}) of (a) **D3**⊂**CBPQT**$^{4+}$, (b) **D2**$^{2+}$⊂**CBPQT**$^{4+}$, and (c) **D1**$^{+}$⊂**CBPQT**$^{4+}$. Note that the CV traces for [2]pseudorotaxanes **D2**$^{2+}$⊂**CBPQT**$^{4+}$ and **D1**$^{+}$⊂**CBPQT**$^{4+}$ display only one reduction peak for the first two-electron reduction process whereas in the case of [2]pseudorotaxane **D3**⊂**CBPQT**$^{4+}$ two individual one-electron reduction peaks are observable. These observations support the hypothesis that upon reduction of the tetracationic **CBPQT**$^{4+}$ ring the 2-isopropylphenyl group slows down the dissociation of the **D3**⊂**CBPQT**$^{(2+)(\bullet+)}$/**CBPQT**$^{2(\bullet+)}$ inclusion complex quite considerably, whereas the 3,5-dimethylpyridinium cation provides relatively easy passage to the **CBPQT**$^{(2+)(\bullet+)}$/**CBPQT**$^{2(\bullet+)}$ ring. The measurements were all performed at ambient temperature and at a concentration of 1.0 mM.

dx.doi.org/10.1021/ja4094204 | J. Am. Chem. Soc. 2013, 135, 18609−18620

experiment. As a consequence, the second $BIPY^{2+}$ unit no longer participates in donor−acceptor interactions and so is reduced at the same potential as the first one. In other words, the 3,5-dimethylpyridinium termini of dumbbell $\mathbf{D2}^{2+}$ fail to provide a sufficiently large energy barrier for the tricationic $\mathbf{CBPQT}^{(2+)(\bullet+)}$ ring to prevent its dethreading. The rapid dethreading is a consequence of the diminished Coulombic repulsion between these two cationic species, $\mathbf{D2}^{2+}$ and $\mathbf{CBPQT}^{(2+)(\bullet+)}$, following reduction and partial neutralization of the charge compared to those of tetracationic $\mathbf{CBPQT}^{4+}$. Increasing the scan rate from 250 to 5000 mV s^{-1} in the CV experiment[28] did not alter the first two-electron reduction of $\mathbf{D2}^{2+}\subset\mathbf{CBPQT}^{4+}$, indicating that the dissociation of the complex under reductive conditions occurs rapidly on the millisecond time scale. A control CV experiment[28] showed that pseudorotaxane analogue $\mathbf{BHEEN}\subset\mathbf{CBPQT}^{4+}$ that lacks any kind of barrier at its termini and that would be expected to undergo rapid and unhindered dissociation, behaves in a manner similar to that of $\mathbf{D2}^{2+}\subset\mathbf{CBPQT}^{4+}$.

Finally, we used CV to investigate (Figure 4c) the behavior of the asymmetric pseudorotaxane $\mathbf{D1}^{+}\subset\mathbf{CBPQT}^{4+}$ under reductive conditions. A single two-electron reduction of the ring to its $\mathbf{CBPQT}^{2(\bullet+)}$ diradical state was observed and is akin to that detected for symmetrical pseudorotaxane $\mathbf{D2}^{2+}\subset\mathbf{CBPQT}^{4+}$ with 3,5-dimethylpyridinium termini. By applying the same logic as we applied to the analysis of the CV of $\mathbf{D2}^{2+}\subset\mathbf{CBPQT}^{4+}$, we reach the conclusion that the ring dissociates rapidly from $\mathbf{D1}^{+}$ on the time scale of the CV experiment. Thus, on the basis of the similar nature of the voltammograms shown in Figure 4b,c, it appears that the course taken by the ring under reductive conditions is governed by the charged terminus of dumbbell $\mathbf{D1}^{+}$. Upon reduction of $\mathbf{D1}^{+}\subset\mathbf{CBPQT}^{4+}$, the [2]pseudorotaxane undergoes rapid mechanostereoselective dissociation as a result of the $\mathbf{CBPQT}^{(2+)(\bullet+)}$ ring slipping over the 3,5-dimethylpyridinium end, thus avoiding the steric hindrance presented by the 2-isopropylphenyl end.

2.5. DFT Calculations. Computational studies based on DFT were performed with a view to gaining further insight into the mechanostereoselectivity of the redox-stimulated threading/dethreading of $\mathbf{D1}^{+}\subset\mathbf{CBPQT}^{4+}$. According to the results of these calculations, the $\mathbf{CBPQT}^{4+}$ ring has to overcome energy barriers ($\Delta E^{\ddagger}$) of 34.3 and 17.2 kcal mol^{-1} (Figure 5a) in order to thread onto dumbbell $\mathbf{D1}^{+}$ from the 3,5-dimethylpyridinium and 2-isopropylphenyl ends, respectively. The theoretical $\Delta E^{\ddagger}$ value for the 2-isopropylphenyl barrier matches well the experimental data, whereas that of the 3,5-dimethylpyridinium end is considerably higher (34.3 vs 22.9 kcal mol^{-1}) than we determined (Figure 2 cf. Figure 5a) using ^{1}H NMR spectroscopy. This discrepancy is most likely an upshot of interactions between ions in solution that were not accounted for by the computational model. In a CD_3CN solution of $\mathbf{D1}^{+}\subset\mathbf{CBPQT}^{4+}$, both $\mathbf{D1}^{+}$ and $\mathbf{CBPQT}^{4+}$ are surrounded by PF_6^{-} counterions that serve to neutralize the positive charges partially, thereby sating the Coulombic repulsion between the two cationic species to some extent.

When we extended our computational studies to the tricationic $\mathbf{CBPQT}^{(2+)(\bullet+)}$ ring, we found that the $\Delta E^{\ddagger}$ values for its dethreading from the 3,5-dimethylpyridinium and 2-isopropylphenyl ends are 38.1 and 28.5 kcal mol^{-1}, respectively (i.e., 31.6 and 22.0 kcal mol^{-1} in threading terms (Figure 5b)). The energy barrier (31.6 kcal mol^{-1}) for the $\mathbf{CBPQT}^{(2+)(\bullet+)}$ ring to slip over the 3,5-dimethylpyridinium end is smaller than that (34.3 kcal mol^{-1}) for the $\mathbf{CBPQT}^{4+}$ ring, a situation that is hardly surprising because the Coulombic repulsion between the reduced ring and the 3,5-dimethylpyridinium end is significantly

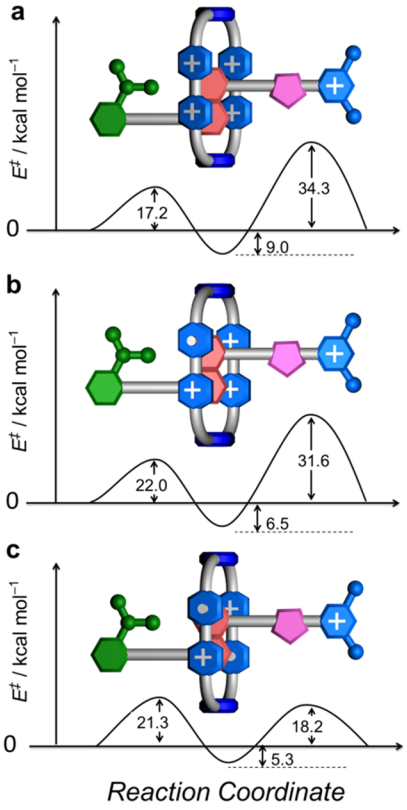

Figure 5. Density functional theory (DFT) calculations. The simplified potential energy curves of the $\mathbf{D1}^{+}\subset\mathbf{CBPQT}^{4+}$ inclusion complex when the macrocycle is in its (a) fully oxidized state, (b) monoradical dicationic state, and (c) diradical dicationic state, as obtained from DFT calculations.

reduced. According to DFT calculations, the energy barrier for the $\mathbf{CBPQT}^{(2+)(\bullet+)}$ ring to slip over the 3,5-dimethylpyridinium end is larger by 9.6 kcal mol^{-1} than that presented by the 2-isopropylphenyl end, an observation that is not consistent with the results obtained from CV experiments. This inconsistency probably arises as a consequence of the overestimation of Coulombic repulsion between the ring and the charged ends of the dumbbell on account of the fact that the effect of counterions is not considered in the calculations. In the case of the dicationic $\mathbf{CBPQT}^{2(\bullet+)}$ ring, the values of $\Delta E^{\ddagger}$ for its dissociation from the 3,5-dimethylpyridinium and 2-isopropylphenyl ends of the $\mathbf{D1}^{+}$ dumbbell are 23.5 and 26.6 kcal mol^{-1}, respectively, which translate (Figure 5c) to peaks 18.2 and 21.3 kcal mol^{-1} above the energy of the noncomplexed components. The results of this calculation are consistent with dissociation of $\mathbf{D1}^{+}\subset\mathbf{CBPQT}^{2(\bullet+)}$ occurring preferentially at the 3,5-dimethylpyridinium end. Although the DFT methods implemented here have failed to predict the precise magnitude of the Coulombic energy barriers, the trends observed for each end of the $\mathbf{D1}^{+}$ dumbbell across the range of **CBPQT** oxidation states matches at least qualitatively the experimental observations that the barrier to threading/dethreading over the 2-isopropylphenyl end group is relatively independent of the oxidation state of the ring whereas the barrier presented by the 3,5-dimethylpyridinium end decreases significantly, and in a stepwise manner, as the ring is oxidized from its tetracationic state to a trication and then to a dication.

2.6. Light-Stimulated Mechanostereoselective Switching. Now that it has been established that, whether it be under the influence of chemical or electrochemical stimuli,

dx.doi.org/10.1021/ja4094204 | J. Am. Chem. Soc. 2013, 135, 18609−18620

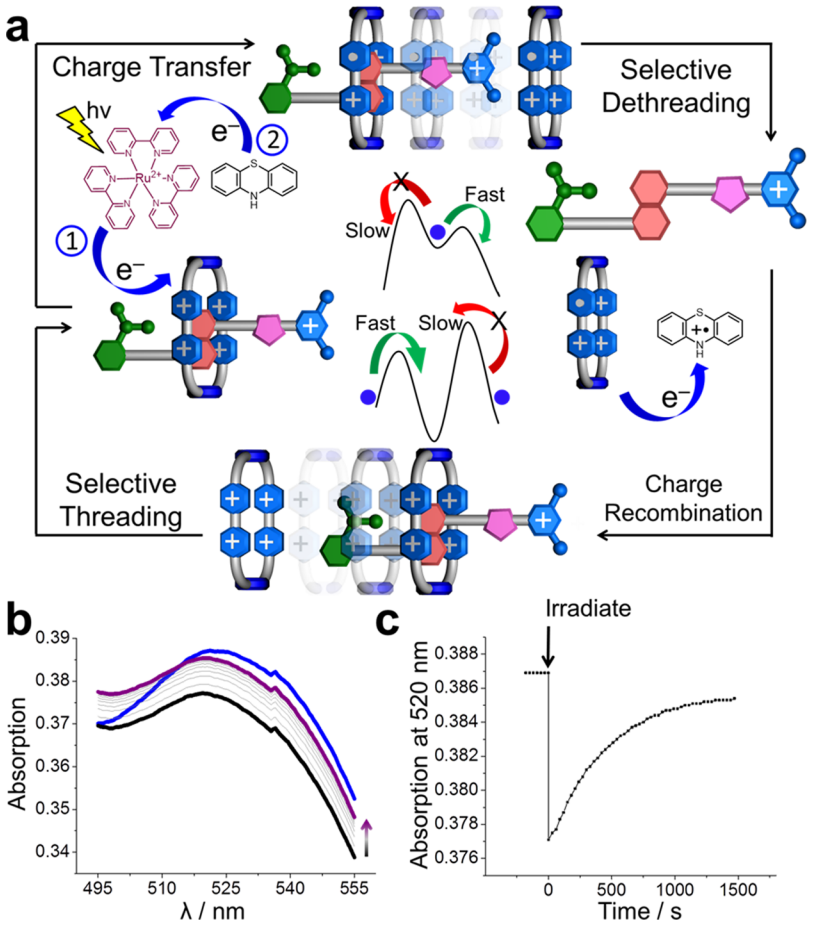

Figure 6. (a) Graphical representation of the mechanism of autonomous mechanostereoselective threading/dethreading of inclusion complex $\mathbf{D1}^{+}\subset\mathbf{CBPQT}^{4+}$ in the presence of $Ru(bpy)_3Cl_2$ and ptz under 450 nm irradiation, where (1) and (2) indicate the order of electron transfer, first from the $Ru(bpy)_3^{2+}$ excited state to the $\mathbf{CBPQT}^{4+}$ ring and then from ptz to the newly formed $Ru(bpy)_3^{3+}$. (b) Partial UV/vis absorption spectra of the MeCN solution of the mixture of $\mathbf{D1}^{+}$, $\mathbf{CBPQT}^{4+}$, $Ru(bpy)_3Cl_2$, and ptz ($[\mathbf{D1}^{+}]_0 = 1.0 \times 10^{-3}$ M, $[\mathbf{CBPQT}^{4+}]_0 = 2.5 \times 10^{-3}$ M, $[Ru(bpy)_3Cl_2] = 2.6 \times 10^{-5}$ M, and [ptz] = 1.7×10^{-3} M) recorded before (blue trace) and 40 s after (black trace) the solution has been irradiated with a laser at 450 nm for 5 min and then after being allowed to stand in the dark for 30 min (purple trace); for full spectra, see Figure S10e. After laser irradiation for 5 min, the spectra were recorded every 40 s in a 1 mm cell-path-length cuvette: selected spectra recorded at intermediate times (gray traces) show a gradual increase in absorption over 30 min, as indicated by the arrow. (c) Absorbance at 520 nm is plotted for all the times measured, showing an increase in the charge-transfer band with an observed rate constant of $k_{obs} = 2.2 \times 10^{-3}$ s^{-1}.

pseudorotaxane $\mathbf{D1}^{+}\subset\mathbf{CBPQT}^{4+}$ undergoes directional threading and dethreading, we relate how we sought (Figure 6) to drive the mechanostereochemical translation process using visible light, a particularly appealing energy source that features prominently in the operation of nature's biochemical machinery.[7] We set out to alter the redox state of the ring in a photoredox reaction mediated by a photosensitizer capable of reducing viologens and selected $Ru(bpy)_3^{2+}$ because it is known[30] to possess a long-lived ^{3}MLCT excited state with a reduction potential of −0.81 V versus the saturated calomel electrode in MeCN. Previously, we employed $Ru(bpy)_3^{2+}$ derivatives to control the minimum-energy coconformation of viologen-containing MIMs.[2Sc,31] On the basis of these previous investigations, we envisaged that the irradiation of a deaerated MeCN solution of $\mathbf{D1}^{+}\subset\mathbf{CBPQT}^{4+}$, $Ru(bpy)_3^{2+}$, and phenothiazine (ptz) with 450 nm light would result in photoinduced electron transfer from the $Ru(bpy)_3^{2+}$ excited state to the $\mathbf{CBPQT}^{4+}$ component of the pseudorotaxane, reducing (Figure 6a) the ring to radical cation $\mathbf{CBPQT}^{(2+)(\bullet+)}$. The ptz plays the role of an electron relay in order to delay back electron transfer by reacting with the $Ru(bpy)_3^{3+}$ to regenerate the initial $Ru(bpy)_3^{2+}$. It has been shown[31b] previously to extend the lifetime of reduced viologens sufficiently to allow the relative motion of the constituent parts of MIMs to occur prior to charge recombination. If the dethreading of reduced [2]pseudorotaxane occurs (Figure 6a) more rapidly than the reaction between $ptz^{\bullet+}$ and $\mathbf{CBPQT}^{(2+)(\bullet+)}$, then the reduced ring will slip over the 3,5-dimethylpyridinium end group into solution before subsequent charge recombination generates free $\mathbf{CBPQT}^{4+}$ and $\mathbf{D1}^{+}$, which should then undergo selective threading by passage of the fully charged ring over the 2-isopropylphenyl terminus. Because the change in the redox state of the $\mathbf{CBPQT}^{4+}$ ring is transient, in principle this mechanism allows the mechanostereoselective translation to proceed autonomously with light as the sole stimulus.

We employed UV/vis spectroscopy in order to monitor (Figure 6b,c) the intensity of the charge-transfer band of the $\mathbf{D1}^{+}\subset\mathbf{CBPQT}^{4+}$ complex centered on 520 nm before and after irradiation with 450 nm light in the presence of $Ru(bpy)_3^{2+}$ and ptz. A deaerated MeCN solution of the mixture in a sealed cuvette was subjected to 450 nm laser irradiation for 5 min and then transferred to a UV/vis spectrometer where it was kept in the dark while a spectrum was recorded every 40 s. A decrease in the absorbance of the charge-transfer band was observed directly after irradiation, before the signal gradually grew almost to its original intensity over a period of 30 min, indicative of dissociation of the

dx.doi.org/10.1021/ja4094204 | J. Am. Chem. Soc. 2013, 135, 18609−18620

pseudorotaxane during the irradiation and subsequent gradual rethreading after charge recombination. Control reactions performed in the absence of either $Ru(bpy)_3^{2+}$ or ptz did not exhibit[28] any marked change in their absorbances at 520 nm. These observations are consistent with the mechanism illustrated in Figure 6a, whereby the flux of light energy drives the system away from its thermal equilibrium as a result of the unidirectional relative motion of the components of $\mathbf{D1}^+\subset\mathbf{CBPQT}^{4+}$.

Pseudorotaxane $\mathbf{D1}^+\subset\mathbf{CBPQT}^{4+}$ essentially acts as a conduit for the dissipation of absorbed light energy imparted through the absorption of a photon by an Ru center, and on account of the flashing ratchet mechanism that is in operation (Figure 1), it undergoes unidirectional dethreading and threading in the process. In principle, this mechanism continues to operate even once a steady state is reached; that is, although the populations of each species will remain static (nonadiabatic equilibrium is established), there will be a net flux around the cycle as shown in Figure 6a in a single direction.[32] It has to be said, however, that although this system is capable of repetitive operation, the work is "undone" at the end of each cycle because the ring returns to its initial state in the bulk solution. Hence, the pseudorotaxane should be regarded as a prototype for (i) polymeric systems in which substrates could be transported over a large distance[3] or (ii) the forerunner of artificial molecular pumps that could create concentration gradients[6−8] or reptitively build up molecules that lie energetically uphill from their starting materials.[33] Realizing such goals will hinge upon devising systems wherein some of the energy input is captured during the redox cycle, for example, by transporting a ring to an environment that is energetically demanding and distant from the starting state. Theory[12a] also dictates that instead of controlling the redox state of an MM using an external energy input, microscopic reversibility can also be overcome in systems in which the MM acts as a catalyst for a pair of coupled redox reactions. Autonomous mechanostereoselective relative translation of the assembly in the present system, therefore, could also be achieved by linking the oxidation and reduction of the $\mathbf{CBPQT}^{4+}$ ring to two separate redox couples.

3. CONCLUSIONS

The findings presented in this article constitute a proof of principle in relation to the operation of a flashing energy ratchet, with the simultaneous juggling of (i) the depth of a potential energy well associated with donor−acceptor interactions in a prototypical [2]pseudorotaxane while (ii) the heights of kinetic energy barriers arising from steric interactions and Coulombic repulsion are raised and lowered under redox control, resulting in the threading of a positively charged ring at the neutral end of the dumbbell on oxidation, followed by the ring's departure from the dumbbell's positively charged end on reduction. That is, oscillation of one component between different redox states changes the relative levels of the energy minima and maxima simultaneously in a two-component supramolecular system, setting up a flashing energy ratchet that allows another component to move relatively in one and only one direction during the association (complexation) and dissociation (decomplexation) of the supramolecular system. From the fundamental perspective of artificial energy ratchets, not only does the unidirectional translation in this two-component supramolecular system occur in response to a single stimulus, which simultaneously controls two kinetic barriers and one thermodynamic well such that microscopic reversibility is overcome, but it (i) is also capable of autonomous translation under the influence of light, which coaxes the system away from equilibrium, (ii) relies solely for its operation on reversible yet stable noncovalent bonding interactions and as such does not necessitate the formation and cleavage of covalent bonds, and (iii) contains a ratchet mechanism driven by a simple change in the redox properties of the component within the supramolecular system that can be controlled electro- and photochemically, making it practically feasible to repeat the operation numerous times without the buildup of byproducts that often hamper the operation of other artificial molecular motors. To ensure that this nonequilibrium system does work, however, it now needs to be taken to the next level of design to capture and store the high-energy states away from equilibrium in order to be able to use them in other ways in an integrated system. Such ratchet-driven transport is employed in the operation of nature's molecular motors to push biological systems away from equilibrium so that they can do their work inside living systems.

4. EXPERIMENTAL SECTION

Full experimental details are provided in the Supporting Information. The most important information is summarized briefly below.

4.1. Dumbbell Synthesis. Dumbbells $\mathbf{D1}\cdot PF_6$, $\mathbf{D2}\cdot 2PF_6$, and **D3** were synthesized according to the synthetic routes shown in Scheme 1. All reagents were purchased from commercial suppliers (Aldrich or Fisher) and used without further purification. $\mathbf{CBPQT}\cdot PF_6$,[34] the bisazide[24] and ditosylate[35] of 1.5-bis[2-(2-hydroxyethoxy)ethoxy]-naphthalene were prepared according to literature procedures. Thin layer chromatography (TLC) was performed on aluminum-backed silica plates (silica gel 60 F254, E. Merck). Column chromatography was carried out on silica gel 60F (Merck 9385, 0.040−0.063 mm). Nuclear magnetic resonance (NMR) spectra were recorded on Bruker Avance 600 and Varian P-Inova 500 spectrometers, with working frequencies of 600 and 500 MHz for ^{1}H and 150 and 125 MHz for ^{13}C nuclei, respectively. Chemical shifts are reported in parts per million relative to the signals corresponding to the residual nondeuterated solvents ($CDCl_3$: δ = 7.26 ppm, CD_3CN: δ = 1.94 ppm). High-resolution mass spectra were obtained either on an Applied Biosystems Voyager DE-PRO MALDI TOF mass spectrometer (HR-TOF) or on a Finnigan LCQ iontrap mass spectrometer (HR-ESI).

4.1.1. $\mathbf{D1}\cdot PF_6$. A solution of **1** (48 mg, 0.1 mmol), 3,5-dimethyl-1-(but-3-ynyl)-pyridinium hexafluorophosphate (31 mg, 0.1 mmol), tris[(1-benzyl-1*H*-1,2,3-triazol-4-yl)methyl]amine (TBTA, 9 mg, 0.017 mmol), and $Cu(MeCN)_4PF_6$ (6 mg, 0.017 mmol) in anhydrous Me_2CO (5 mL) was stirred for 24 h at room temperature. The solvent was then removed in vacuo, and the resulting solid was purified by column chromatography [SiO_2: 2 M NH_4Cl/MeOH/$MeNO_2$ (12:7:1)]. The light-yellow fraction was collected and concentrated under reduced pressure. The solid residue was dissolved in H_2O, followed by the addition of NH_4PF_6 (2 g). The resulting mixture was extracted with CH_2Cl_2 (3 × 100 mL), and the combined organic phases were washed three times with saturated aqueous NaCl solution (3 × 100 mL). After drying ($MgSO_4$), the solvent was removed in vacuo to afford desired product $\mathbf{D1}\cdot PF_6$ (60 mg, 76%) as a light-yellow oil. ^{1}H NMR (600 MHz, CD_3CN): δ = 8.12 (s, 2H), 7.99 (s, 1H), 7.82 (d, *J* = 8.5 Hz, 1H), 7.75 (d, *J* = 8.5 Hz, 1H), 7.62 (s, 1H), 7.39 (t, *J* = 8.5 Hz, 1H), 7.37 (t, *J* = 8.5 Hz, 1H), 7.22 (dd, *J* = 8.5, 1.5 Hz, 1H), 7.14 (td, *J* = 7.5, 1.5 Hz, 1H), 6.96−6.91 (m, 4H), 4.55−4.52 (m, 4H), 4.29 (t, *J* = 6.0 Hz, 2H), 4.23 (t, *J* = 6.0 Hz, 2H), 4.17 (t, *J* = 6.0 Hz, 2H), 4.03 (t, *J* = 6.0 Hz, 2H), 3.98 (t, *J* = 6.0 Hz, 2H), 3.95 (t, *J* = 6.0 Hz, 2H), 3.92 (t, *J* = 6.0 Hz, 2H), 3.32 (septet, *J* = 7.0 Hz, 1H), 3.18 (t, *J* = 6.0 Hz, 2H), 2.36 (s, 6H), 1.16 (d, *J* = 7.0 Hz, 6H). ^{13}C NMR (150 MHz, CD_3CN): δ = 155.7, 154.0, 153.8, 146.3, 140.9, 138.4, 136.5, 126.3, 126.1, 126.0, 125.6, 125.2, 125.1, 123.0, 120.4, 113.8, 113.6, 111.4, 105.5, 105.4, 69.4, 69.1, 68.8, 68.8, 67.8, 67.5, 67.4, 60.1, 49.5, 26.3, 21.6, 16.9. MS (MALDI−TOF) calcd for m/z = 639.355 $[M - PF_6]^+$, found m/z = 639.508.

4.1.2. $\mathbf{D2}\cdot 2PF_6$. A solution of **2** (38 mg, 0.1 mmol), 3,5-dimethyl-1-(but-3-ynyl)-pyridinium hexafluorophosphate (61 mg, 0.2 mmol), TBTA (9 mg, 0.017 mmol), and $Cu(MeCN)_4PF_6$ (6 mg, 0.017 mmol) in anhydrous Me_2CO (5 mL) was stirred for 24 h at room temperature. The solvent was then removed in vacuo, and the solid residue was purified by column chromatography [SiO_2: 2 M NH_4Cl/MeOH/$MeNO_2$ (12:7:1)].

dx.doi.org/10.1021/ja4094204 | J. Am. Chem. Soc. 2013, 135, 18609−18620

The light-yellow fraction was collected and concentrated under reduced pressure. The solid residue was dissolved in H_2O, followed by the addition of NH_4PF_6 (2 g). The resulting mixture was extracted with CH_2Cl_2 (3 × 100 mL), and the combined organic phases were washed three times with saturated aqueous NaCl solution (3 × 100 mL). After drying ($MgSO_4$), the solvent was removed in vacuo to afford desired product **D2**·PF_6 (75 mg, 76%) as a light-yellow oil. ^{1}H NMR (500 MHz, CD_3CN): δ = 8.15 (s, 4H), 7.99 (s, 2H), 7.70 (d, J = 8.5 Hz, 2H), 7.66 (s, 2H), 7.38 (t, J = 8.5 Hz, 2H), 6.89 (d, J = 8.5 Hz, 2H), 4.57 (t, J = 6.0 Hz, 4H), 4.52 (t, J = 6.0 Hz, 4H), 4.19 (t, J = 6.0 Hz, 4H), 3.95 (t, J = 6.0 Hz, 4H), 3.90 (t, J = 6.0 Hz, 4H), 3.21 (t, J = 6.0 Hz, 4H), 2.35 (s, 12H). ^{13}C NMR (125 MHz, CD_3CN): δ = 153.8, 146.3, 140.9, 138.4, 126.0, 125.3, 123.2, 113.7, 105.6, 68.8, 68.8, 67.5, 60.1, 49.6, 26.3, 16.9. ESI-HRMS calcd for m/z = 851.3597 $[M - PF_6]^+$, found m/z = 851.3590.

4.1.3. ***D3***. Compound **3** (64 mg, 0.1 mmol), 2-isopropylphenol (27 mg, 0.2 mmol), and K_2CO_3 (138 mg, 1 mmol) were added to a round-bottomed flask (250 mL) containing dry DMF (50 mL). The reaction mixture was stirred at 80 °C for 8 h. After cooling to room temperature, the solution was poured into H_2O (200 mL). The resulting mixture was extracted with EtOAc (3 × 20 mL), and the combined organic phases were washed three times with saturated aqueous NaCl solution (3 × 100 mL). After drying ($MgSO_4$), the solvent was removed in vacuo, and the resulting residue was purified by column chromatography [SiO_2: hexanes/EtOAc (80:20)] to afford desired product **D3** (44 mg, 75%) as a light-yellow oil. ^{1}H NMR (500 MHz, $CDCl_3$): δ = 7.87 (d, J = 8.5 Hz, 2H), 7.32 (t, J = 8.5 Hz, 2H), 7.21 (dd, J = 7.5, 1.5 Hz, 2H), 7.14 (td, J = 8.0, 1.5 Hz, 2H), 6.93 (td, J = 8.0, 1.5 Hz, 2H), 6.86–6.84 (m, 2H), 4.32 (t, J = 5.0 Hz, 4H), 4.19 (t, J = 5.0 Hz, 4H), 4.09 (t, J = 5.0 Hz, 4H), 4.03 (t, J = 5.0 Hz, 4H), 3.36 (septet, J = 7.0 Hz, 2H), 1.20 (d, J = 7.0 Hz, 12H). ^{13}C NMR (125 MHz, $CDCl_3$): δ = 156.0, 154.3, 137.3, 126.8, 126.5, 126.1, 126.1, 125.1, 120.9, 114.7, 111.5, 105.6, 70.3, 70.0, 68.0, 67.8, 26.9, 22.7. MS (MALDI–TOF) calcd for m/z = 572.312 $[M]^+$, found m/z = 572.461.

4.2. Formation of Pseudorotaxanes under Oxidative Conditions. *4.2.1.* ***D1**·PF_6⊂**CBPQT**·PF_6*. UV/vis spectroscopy, performed on a Varian 100-Bio UV/vis spectrophotometer in MeCN at room temperature, was employed to evaluate the kinetic parameters controlling the association and dissociation of pseudorotaxane **D1**$^+$⊂**CBPQT**$^{4+}$. The intensity of the absorbance at 520 nm resulting from charge transfer was used as a measure of the concentration of the pseudorotaxane and monitored as a function of time. Growth of the absorbance at 520 nm in the second time range was recorded (Figure S6) for the formation of the **D1**$^+$⊂**CBPQT**$^{4+}$ inclusion complex. The concentration of **CBPQT**·PF_6 was varied, and the pseudo-first-order rate constants, k_{obs}, were calculated to be 1.10×10^{-2}, 1.39×10^{-2}, 1.68×10^{-2}, 2.10×10^{-2}, 2.47×10^{-2}, 2.88×10^{-2}, 3.27×10^{-2}, and 3.67×10^{-2} s^{-1} when the corresponding concentrations of **CBPQT**·PF_6 were 4.5×10^{-3}, 6.8×10^{-3}, 9.1×10^{-3}, 11.3×10^{-3}, 13.6×10^{-3}, 15.9×10^{-3}, 18.2×10^{-3}, and 20.5×10^{-2} M, respectively. On the basis of these data, a plot (Figure 3c) of k_{obs} versus the concentration of **CBPQT**·PF_6 yields a rate of association of k_f = 1.6 ± 0.04 M^{-1} s^{-1} and a rate of dissociation of $k_b = 2.7 \pm 0.5 \times 10^{-3}$ s^{-1}. The ratio of k_f/k_b (5.9×10^2 M^{-1}) is consistent with the thermodynamic equilibrium constant (6.0×10^2 M^{-1}) determined by ^{1}H NMR spectroscopy. On the basis of these data, $\Delta G^{\ddagger}_{threading}$ = 17.2 kcal mol^{-1} and $\Delta G^{\ddagger}_{dethreading}$ = 21.0 kcal mol^{-1} were deduced.

4.2.2. ***D2**·2PF_6⊂**CBPQT**·PF_6*. ^{1}H NMR spectroscopy, performed on a Bruker Avance 500 spectrometer, was employed to evaluate the kinetic parameters controlling the association and dissociation of pseudorotaxane **D2**$^{2+}$⊂**CBPQT**$^{4+}$. After the pseudorotaxane reached equilibrium, a binding constant of K = 180 M^{-1} was obtained by using the expression $K = [\mathbf{D2}{\cdot}2PF_6{\subset}\mathbf{CBPQT}{\cdot}PF_6]/([\mathbf{D2}{\cdot}2PF_6][\mathbf{CBPQT}{\cdot}PF_6])$, in which [**D2**·2$PF_6$⊂**CBPQT**·$PF_6$], [**D2**·2$PF_6$], and [**CBPQT**·$PF_6$] represent the concentrations of complex **D2**·2PF_6⊂**CBPQT**·PF_6, dumbbell **D2**·2PF_6, and ring **CBPQT**·PF_6 at equilibrium, respectively. From an initial concentration of dumbbell [**D2**$^{2+}$] of 1.2×10^{-3} M, the relative integration of peaks corresponding to the free dumbbell and pseudorotaxane was used (Figure 2d) as a measure of the concentration of the pseudorotaxane and monitored as a function of time. The initial concentration of **CBPQT**·PF_6 was varied, and the pseudo-first-order rate constants, k_{obs}, were calculated to be 4.00×10^{-6}, 5.34×10^{-6}, 5.74×10^{-6}, 6.14×10^{-6}, and 1.03×10^{-5} s^{-1} when the corresponding concentrations of **CBPQT**·PF_6 were 2.0×10^{-2}, 2.7×10^{-2}, 3.0×10^{-2}, 3.3×10^{-2}, and 4.5×10^{-2}, respectively. On the basis of these data, a plot (Figure 2e) of k_{obs} versus the concentration of **CBPQT**·PF_6 yields a rate of association of $k_f = 2.0 \pm 0.2 \times 10^{-4}$ M^{-1} s^{-1}. By using the equation $K = k_f/k_b$, a rate of dissociation of $k_b = 1.1 \pm 1.1 \times 10^{-6}$ s^{-1} can be deduced. The slow rates for both threading and dethreading result from the Coulombic repulsion between the pyridinium-based stopper and the **CBPQT**·PF_6 ring. On the basis of these data, $k_{threading} = 1.0 \times 10^{-4}$ M^{-1} s^{-1} and $k_{dethreading} = 5.6 \times 10^{-7}$ s^{-1} can be deduced by using the relationships $k_{threading} = k_f/2$ and $k_{dethreading} = k_b/2$, given that threading/detheading could occur at both ends of the dumbbell. The free energies of activation for the threading ($\Delta G^{\ddagger}_{threading}$ = 22.9 kcal mol^{-1}) and dethreading ($\Delta G^{\ddagger}_{dethreading}$ = 25.9 kcal mol^{-1}) are calculated by using the relationships $\Delta G^{\ddagger} = -RT\ln(kh/k_BT)$, where k, R, h, and k_B correspond to the rate constants for threading or dethreading, and the gas, Planck, and Boltzmann constants, respectively.

4.2.3. ***D3**⊂**CBPQT**·PF_6*. The kinetics of **D3**⊂**CBPQT**$^{4+}$ formation were monitored (Figure S7) by UV/vis spectroscopy according to a procedure similar to that used for **D1**$^+$⊂**CBPQT**$^{4+}$.[28] The plot of k_{obs} versus the concentration of **CBPQT**·PF_6 (Figure S7i) yielded a rate of association of $k_f = 5.71 \pm 0.33$ M^{-1} s^{-1} and a rate of dissociation of $k_b = 8.84 \pm 0.42 \times 10^{-3}$ s^{-1}. On the basis of these data, $\Delta G^{\ddagger}_{threading}$ = 16.9 kcal mol^{-1} and $\Delta G^{\ddagger}_{dethreading}$ = 20.6 kcal mol^{-1} were deduced. The close agreement of the observed kinetics of threading and dethreading for **CBPQT**$^{4+}$ with both **D1**$^+$ and **D3** is consistent with our proposal of the directional threading of **CBPQT**$^{4+}$ onto **D1**$^+$ via the 2-isopropylphenyl terminus under oxidative conditions.

4.3. Dissociation of Pseudorotaxanes under Reductive Conditions. *4.3.1. Chemical Reduction.* Zn dust was added to a solution of **D2**·2PF_6⊂**CBPQT**·PF_6 in deaerated MeCN (5 mM) under an Ar atmosphere. The mixture was stirred for 5 min, during which time it acquired a deep blue color indicative of bipyridinium-centered radical formation before the excess Zn powder was removed by filtration through a syringe tip filter. The solution was then exposed to air, resulting in a color change from deep blue to pale yellow, suggesting that pseudorotaxane **D2**$^{2+}$⊂**CBPQT**$^{4+}$ had undergone dissociation. Analysis by ^{1}H NMR spectroscopy (Figure 2b,c) verified the complete decomplexation to a 1:1 mixture of **CBPQT**$^{4+}$ and **D2**$^{2+}$. The chemical reduction of asymmetric complex **D1**·PF_6⊂**CBPQT**·PF_6 was also appraised by employing to the same method. ^{1}H NMR spectra recorded (Figure S4) before and after a reduction/oxidation cycle were found to be identical on account of the rapid reformation of the pseudorotaxane under oxidative conditions.

4.3.2. Electrochemical Reduction. CV experiments were carried out at room temperature in argon-purged solutions of MeCN with a Gamry Multipurpose instrument (Reference 600) interfaced to a PC. A glassy carbon working electrode (0.071 cm^2) was used, and its surface was polished routinely with a 0.05 μm alumina–water slurry on felt immediately before use. The counter electrode was a Pt coil, and the reference electrode was Ag/AgCl. The concentrations of the sample and supporting electrolyte (Bu_4NPF_6) were 1.0×10^{-3} and 0.1 mol L^{-1}, respectively. CV traces (second scan, 200 mV s^{-1}) for **D1**·PF_6⊂**CBPQT**·PF_6, **D2**·2PF_6⊂**CBPQT**·PF_6, and **D3**⊂**CBPQT**$^{4+}$ are shown in Figure 4. A spectroelectrochemical experiment using a 1:2:2 mixture of **CBPQT**$^{4+}$ (1.0×10^{-3} M in MeCN), **D1**$^+$, and methyl viologen (**V**$^{2+}$) showed (Figure S8) characteristic maximum absorptions indicative of $(BIPY^{\bullet+})_2$ radical dimers (λ_{max} = 560 nm, 1080 nm), demonstrating that the reduction of **CBPQT**$^{4+}$ and **V**$^{2+}$ leads to the formation of a **V**$^{\bullet+}$⊂**CBPQT**$^{2(\bullet+)}$ trisradical complex and the dissociation of **D1**$^+$⊂**CBPQT**$^{4+}$. Oxidation of the BIPY$^{\bullet+}$ radicals back to their fully oxidized states leads to the recovery of the initial charge-transfer band of **D1**$^+$⊂**CBPQT**$^{4+}$. CV traces for three control compounds can be found in Figure S11, and the variable scan rate (50 to 5000 mV s^{-1}) CV for **D2**$^{2+}$⊂**CBPQT**$^{4+}$ can be found in Figure S12.

4.3.3. Photochemical Reduction. A deaerated MeCN solution of pseudorotaxane **D1**·PF_6 (1.0×10^{-3} M), **CBPQT**·PF_6 (2.5×10^{-3} M), $Ru(bpy)_3Cl_2$ (2.6×10^{-5} M), and ptz (1.7×10^{-3} M) in a sealed 1 mm cell-path-length cuvette was irradiated for 5 min with 450 nm light

(~5 mL/pluse) from the output of an optical parametric oscillator (Continuum Panther) pumped by the frequency-tripled output of a Nd-YAG laser (Continuum Precision II 8000) operating at 10 Hz. After irradiation, the cuvette was transferred to a UV/vis spectrometer, and the change in intensity of the absorbance at 520 nm resulting from charge transfer between $\mathbf{D1}^+$ and $\mathbf{CBPQT}^{4+}$ was monitored as it increased over time, with spectra recorded at 40 s intervals. Growth in the charge-transfer band over 30 min was observed (Figure 6) with $k_{obs} = 2.2 \times 10^{-3}$ s^{-1}. UV/vis spectra from control experiments conducted in the absence of either $Ru(bpy)_3Cl_2$ or ptz can be found in Figure S9, and data from an experiment in which a pyridinium-terminated dumbbell $\mathbf{D2}'\cdot 2PF_6$ was used in place of $\mathbf{D1}\cdot PF_6$ can be found in Figure S10.

4.4. Computational Methods. Scans of the potential energy surfaces for pseudorotaxanes $\mathbf{D1}^+\subset\mathbf{CBPQT}^{(n+)}$ as the ring moves along the vector of the dumbbell component were carried out for three different oxidation states ($n = 2$, 3, and 4). The z coordinate of a point on $\mathbf{D1}^+$, either the N atom of the pyridinium ring or the central C atom of the isopropyl group (identified in the atomic coordinates[28]), was constrained relative to the center of $\mathbf{CBPQT}^{(n+)}$, which was defined as the center point among its four methylene C atoms. Geometries were optimized in the Poisson–Boltzmann solvation model[36] for acetonitrile ($\varepsilon = 37.5$ and $R_0 = 2.18$ Å) at the level of M06-HF/6-31G* with Jaguar 7.5.[37] At infinite separation, the $\mathbf{CBPQT}^{(n+)}$ rings, fully dissociated from the dumbbell unit, favor the encapsulation of two MeCN molecules. The binding energies of $\mathbf{D1}^+\subset\mathbf{CBPQT}^{(n+)}$ complexes were corrected by subtracting the energetic cost of removing two MeCN solvent molecules from the cavity of $\mathbf{CBPQT}^{(n+)}$, which are 9.9, 8.9, and 6.0 kcal/mol for $n = 2$, 3, and 4, respectively. A list of atomic coordinates of transition states and ground states, along with their corresponding energies, are provided in the Supporting Information.

■ ASSOCIATED CONTENT

Supporting Information

Detailed synthesis procedures and characterization (NMR and HRMS) data for all compounds. Spectroscopic (NMR and UV/vis) and electrochemical (CV) characterization of the pseudorotaxane complexes. This material is available free of charge via the Internet at http://pubs.acs.org.

■ AUTHOR INFORMATION

Corresponding Author

stoddart@northwestern.edu

Notes

The authors declare no competing financial interest.

■ ACKNOWLEDGMENTS

This work was supported by the Non-Equilibrium Energy Center (NERC), which is an Energy Frontier Research Center (EFRC) funded by the U.S. Department of Energy, Office of Science, Office of Basic Energy Sciences award DE-SC0000989. M.R.W., R.M.Y., D.T.C., and S.M.D. are supported by the Argonne Northwestern Solar Energy Research (ANSER) Center, which is an EFRC funded by the DOE-BES under award DE-SC0001059 (light-driven experiments). W.G.L. and W.A.G. are supported by the National Science Foundation (NSF) (CMMI-1120890 and EFRI-ODISSEI-1332411). W.A.G. is also supported by the World Class University (WCU) Program (R-31-2008-000-10055-0) funded by the Ministry of Education, Science and Technology, Republic of Korea. H.L. is thankful for a Chinese Government Award for Outstanding Self-Financed Students Abroad. P.R.M thanks the US-UK Fulbright Commission for an All-Disciplines Scholar Award. A.C.F. acknowledges support from a National Science Foundation (NSF) Graduate Research Fellowship. C.K. thanks the Royal Society in the U.K. for support as a Newton Fellow Alumnus.

■ REFERENCES

(1) *Molecular Motors*; Schliwa, M., Ed.; Wiley-VCH: Weinheim, Germany, 2003.

(2) (a) Boyer, P. D. *Angew. Chem., Int. Ed.* **1998**, *37*, 2296. (b) Walker, J. E. *Angew. Chem., Int. Ed.* **1998**, *37*, 2308.

(3) Hirokawa, N.; Noda, Y.; Tanaka, Y.; Niwa, S. *Nat. Rev. Mol. Cell Bio.* **2009**, *10*, 682.

(4) Berg, J. S.; Powell, B. C.; Cheney, R. E. *Mol. Biol. Cell* **2001**, *12*, 780.

(5) Sowa, Y.; Berry, R. M. *Q. Rev. Biophys.* **2008**, *41*, 103.

(6) Wright, E. M.; Loo, D. D. F.; Hirayama, B. A. *Physiol. Rev.* **2011**, *91*, 733.

(7) Gai, F.; Hasson, K. C.; McDonald, J. C.; Anfinrud, P. A. *Science* **1998**, *279*, 1886.

(8) (a) Skou, J. C. *Angew. Chem., Int. Ed.* **1998**, *37*, 2321. (b) Inoue, K.; Ono, H.; Abe-Yoshizumi, R.; Yoshizawa, S.; Ito, H.; Kogure, K.; Kandori, H. *Nat. Commun.* **2013**, *4*, 1678.

(9) (a) Astumian, R. D. *Sci. Am.* **2001**, *285*, 56. (b) Beausang, J. F.; Shroder, D. Y.; Nelson, P. C.; Goldman, Y. E. *Biophys. J.* **2013**, *104*, 1263.

(10) (a) Astumian, R. D. *Science* **1997**, *276*, 917. (b) Bier, M. *Contemp. Phys.* **1997**, *38*, 371. (c) Parrondo, J. M. R.; De Cisneros, B. J. *Appl. Phys. A: Mater. Sci. Process.* **2002**, *75*, 179. (d) Reimann, P.; Hänggi, P. *Appl. Phys. A: Mater. Sci. Process.* **2002**, *75*, 169. (e) Astumian, R. D.; Derényi, I. *Eur. Biophys. J.* **1998**, *27*, 474.

(11) Astumian, R. D. *Nat. Nanotechnol.* **2012**, *7*, 684.

(12) (a) Coskun, A.; Banaszak, M.; Astumian, R. D.; Stoddart, J. F.; Grzybowski, B. A. *Chem. Soc. Rev.* **2012**, *41*, 19. (b) *Molecular Devices and Machines: Concepts and Perspectives for the Nanoworld*; Balzani, V., Venturi, M., Credi, A., Eds.; Wiley-VCH: Weinheim, Germany, 2008. (c) Collin, J.-P.; Heitz, V.; Sauvage, J.-P. *Top. Curr. Chem.* **2005**, *262*, 29. (d) Kay, E. R.; Leigh, D. A.; Zerbetto, F. *Angew. Chem., Int. Ed.* **2007**, *46*, 72. (e) Stoddart, J. F. *Chem. Soc. Rev.* **2009**, *38*, 1802. (f) Vogelsberg, C. S.; Garcia-Garibay, M. A. *Chem. Soc. Rev.* **2012**, *41*, 1892.

(13) For selected examples, see (a) Krishnan, Y.; Simmel, F. C. *Angew. Chem., Int. Ed.* **2011**, *50*, 3124. (b) Bath, J.; Turberfield, A. J. *Nat. Nanotechnol.* **2007**, *2*, 275. (c) Lu, C. H.; Cecconello, A.; Elbaz, J.; Credi, A.; Willner, I. *Nano Lett.* **2013**, *13*, 2303.

(14) For a recent review see Michl, J.; Sykes, E. C. H. *ACS Nano* **2009**, *3*, 1042.

(15) (a) Leigh, D. A.; Wong, J. K. Y.; Dehez, F.; Zerbetto, F. *Nature* **2003**, *424*, 174. (b) Hernández, J. V.; Kay, E. R.; Leigh, D. A. *Science* **2004**, *306*, 1532.

(16) (a) Kelly, T. R.; De Silva, H.; Silva, R. A. *Nature* **1999**, *401*, 150. (b) Fletcher, S. P.; Dumur, F.; Pollard, M. M.; Feringa, B. L. *Science* **2005**, *310*, 80. (c) Perera, U. G. E.; Ample, E. F.; Kersell, H.; Zhang, Y.; Vives, G.; Echeverria, J.; Grisolia, M.; Rapenne, G.; Joachim, C.; Hla, S.-W. *Nat. Nanotechnol.* **2013**, *8*, 46.

(17) For selected examples, see (a) Koumura, N.; Zijlstra, R. W. J.; van Delden, R. A.; Harada, N.; Feringa, B. L. *Nature* **1999**, *401*, 152. (b) Eelkema, R.; Pollard, M. M.; Vicario, J.; Katsonis, N.; Serrano Ramon, B.; Bastiaansen, C. W. M.; Broer, D. F.; Feringa, B. L. *Nature* **2006**, *440*, 163. (c) Ruangsupapichat, N.; Pollard, M. M.; Harutyunyan, S. R.; Feringa, B. L. *Nat. Chem.* **2011**, *3*, 53. (d) Wang, J. B.; Feringa, B. L. *Science* **2011**, *331*, 1429. (e) Kudernac, T.; Ruangsupapichat, N.; Parschau, M.; Maciá, B.; Katsonis, N.; Harutyunyan, S. R.; Ernst, K.-H.; Feringa, B. L. *Nature* **2011**, *479*, 208. For a review, see (f) Feringa, B. L. *J. Org. Chem.* **2007**, *72*, 6635.

(18) (a) Chatterjee, M. N.; Kay, E. R.; Leigh, D. A. *J. Am. Chem. Soc.* **2006**, *128*, 4058. (b) Serreli, V.; Lee, C. F.; Kay, E. R.; Leigh, D. A. *Nature* **2007**, *445*, 523. (c) Alvarez-Pérez, M.; Goldup, S. M.; Leigh, D. A.; Slawin, A. M. Z. *J. Am. Chem. Soc.* **2008**, *130*, 1836. (d) Carlone, A.; Goldup, S. M.; Lebrasseur, N.; Leigh, D. A.; Wilson, A. *J. Am. Chem. Soc.* **2012**, *134*, 8321.

(19) (a) Baroncini, M.; Silvi, S.; Venturi, M.; Credi, A. *Angew. Chem., Int. Ed.* **2012**, *51*, 4223. (b) Arduini, A.; Bussolati, R.; Credi, A.; Monaco, S.; Secchi, A.; Silvi, S.; Venturi, M. *Chem.—Eur. J.* **2012**, *18*, 16203.

(20) (a) von Delius, M.; Geertsema, E. M.; Leigh, D. A. *Nat. Chem.* **2010**, *2*, 96. (b) von Delius, M.; Geertsema, E. M.; Leigh, D. A.; Tang, D.-T. D. *J. Am. Chem. Soc.* **2010**, *132*, 16134. (c) Barrell, M. J.; Campaña, A. G.; von Delius, M.; Geertsema, E. M.; Leigh, D. A. *Angew. Chem., Int. Ed.* **2011**, *50*, 285. (d) von Delius, M.; Leigh, D. A. *Chem. Soc. Rev.* **2011**, *40*, 3656.

(21) Green, J. E.; Choi, J. W.; Boukai, A.; Bunimovich, Y.; Johnston-Halperin, E.; DeIonno, E.; Luo, Y.; Sheriff, B. A.; Xu, K.; Shin, Y. S.; Tseng, H.-R.; Stoddart, J. F.; Heath, J. R. *Nature* **2007**, *445*, 414.

(22) Odell, B.; Reddington, M. V.; Slawin, A. M. Z.; Spencer, N.; Stoddart, J. F.; Williams, D. J. *Angew. Chem., Int. Ed. Engl.* **1988**, *27*, 1547.

(23) The intermediate species that govern the directional threading and dethreading of the asymmetric [2]pseudorotaxane are transient as a direct consequence of the mechanism of operation. It is not possible, therefore, to trap and characterize the intermediates fully. Dethreading of the **CBPQT**$^{4+}$ ring under reduced conditions occurs on a relatively short time scale—on the order of milliseconds based on CV data—whereas the reduction of the **CBPQT**$^{4+}$ ring in the [2]pseudorotaxane, by either electrochemical or chemical means, often occurs on a relatively longer time scale (ref 25c) as a result of trace amounts of O_2 in the system or is limited by the diffusion of the reductant. As such, methods that could have been employed to monitor the system directly, such as stop-flow UV/vis spectroscopy, would inevitably be subject to substantial experimental errors, so model studies, performed using threads with similar structures and under similar conditions, were pursued as an alternative approach because they are considered to represent the most reliable means by which to probe the behavior of the asymmetric pseudorotaxane with a minimum number of systematic errors.

(24) Zhu, Z.; Fahrenbach, A. C.; Li, H.; Barnes, J. C.; Liu, Z.; Dyar, S. M.; Zhang, H.; Lei, J.; Carmieli, R.; Sarjeant, A. A.; Stern, C. L.; Wasielewski, M. R.; Stoddart, J. F. *J. Am. Chem. Soc.* **2012**, *134*, 11709.

(25) (a) Trabolsi, A.; Khashab, N.; Fahrenbach, A. C.; Friedman, D. C.; Colvin, M. T.; Cotí, K. K.; Benitez, D.; Tkatchouk, E.; Olsen, J.-C.; Belowich, M. E.; Carmielli, R.; Khatib, H. A.; Goddard, W. A., III; Wasielewski, M. R.; Stoddart, J. F. *Nat. Chem.* **2010**, *2*, 42. (b) Li, H.; Fahrenbach, A. C.; Dey, S. V.; Basu, S.; Trabolsi, A.; Zhu, Z.; Botros, Y. Y.; Stoddart, J. F. *Angew. Chem., Int. Ed.* **2010**, *49*, 8260. (c) Li, H.; Fahrenbach, A. C.; Coskun, A.; Zhu, Z.; Barin, G.; Zhao, Y.; Botros, Y. Y.; Sauvage, J.-P.; Stoddart, J. F. *Angew. Chem., Int. Ed.* **2011**, *50*, 6782. (d) Li, H.; Zhao, Y.-L.; Fahrenbach, A. C.; Kim, S.-Y.; Paxton, W. F.; Stoddart, J. F. *Org. Biomol. Chem.* **2011**, *9*, 2240. (e) Fahrenbach, A. C.; Zhu, Z.; Cao, D.; Liu, W.-G.; Li, H.; Dey, S. K.; Basu, S.; Trabolsi, A.; Botros, Y. Y.; Goddard, W. A., III; Stoddart, J. F. *J. Am. Chem. Soc.* **2012**, *134*, 16275. (f) Fahrenbach, A. C.; Sampath, S.; Late, D. J.; Barnes, J. C.; Kleinman, S. L.; Valley, N.; Hartlieb, K. J.; Liu, Z.; Dravid, V. P.; Schatz, G. C.; Van Duyne, R. P.; Stoddart, J. F. *ACS Nano* **2012**, *6*, 9964. (g) Fahrenbach, A. C.; Barnes, J. C.; Lanfranchi, D. A.; Li, H.; Coskun, A.; Gassensmith, J. J.; Liu, Z.; Benítez, D.; Trabolsi, A.; Goddard, W. A., III; Elhabiri, M.; Stoddart, J. F. *J. Am. Chem. Soc.* **2012**, *134*, 3061. (h) Barnes, J. C.; Fahrenbach, A. C.; Cao, D.; Dyar, S. M.; Frasconi, M.; Giesener, M. A.; Benítez, D.; Tkatchouk, E.; Chernyashevskyy, O.; Shin, W. H.; Li, H.; Sampath, S.; Stern, C. L.; Sarjeant, A. A.; Hartlieb, K. J.; Liu, Z.; Carmieli, R.; Botros, Y. Y.; Choi, J. W.; Slawin, A. M. Z.; Ketterson, J. B.; Wasielewski, M. R.; Goddard, W. A., III; Stoddart, J. F. *Science* **2013**, *339*, 429. (i) Li, H.; Zhu, Z.; Fahrenbach, A. C.; Savoie, B. M.; Ke, C.; Barnes, J. C.; Lei, J.; Zhao, Y.-L.; Lilley, L. M.; Marks, T. J.; Ratner, M. A.; Stoddart, J. F. *J. Am. Chem. Soc.* **2013**, *135*, 456.

(26) Although repulsion between like charges of the **CBPQT**$^{4+}$ ring and the 3,5-dimethylpyridinium end group is tempered somewhat by solvation and ion pairing with hexafluorophosphate anions, DFT calculations indicate that electrostatic repulsion is still the dominant factor in determining the heights of the energy barriers that must be overcome in order to thread/dethread at this terminus. A control experiment conducted using a neutral analog, bearing a 3,5-dimethylphenyl group in place of the 3,5-dimethylpyridinium unit, also supports this rationlization. Indeed, the energy barrier for the ring undergoing threading/dethreading was found to be reduced to such an extent that it is too low to be measured, even at −45 °C.

(27) Ashton, P. R.; Ballardini, R.; Balzani, V.; Boyd, S. E.; Credi, A.; Gandolfi, M. T.; Gómez-López, M.; Iqbal, S.; Philp, D.; Preece, J. A.; Prodi, L.; Ricketts, H. G.; Stoddart, J. F.; Tolley, M. S.; Venturi, M.; White, A. J. P.; Williams, D. J. *Chem.—Eur. J.* **1997**, *3*, 152.

(28) See the Supporting Information for further details.

(29) Although both $BIPY^{2+}$ units of pseudorotaxanes **D1**·PF_6⊂**CBPQT**·PF_6, **D2**·$2PF_6$⊂**CBPQT**·PF_6, and **D3**⊂**CBPQT**·PF_6 appear to be chemically identical to one another by ^{1}H NMR spectroscopy, at any given instant the electrons in the HOMO of the DNP unit donate only to the LUMO of one of the two $BIPY^{2+}$ units in the **CBPQT**$^{4+}$ ring. The apparent equivalence observed by ^{1}H NMR spectroscopy is a result of rapid equilibration on the ^{1}H NMR time scale. On the time scale of the CV experiments, these two $BIPY^{2+}$ units are not chemically identical (i.e., the one that is interacting with DNP is less electron deficient than the one that is not interacting). Similar stepwise two-electron reduction has been observed when the **CBPQT**$^{4+}$ ring encapsulates other electron-rich heteroaromatics in the dumbbell component of rotaxanes. See Flood, A. H.; Nygaard, S.; Laursen, B. W.; Jeppesen, J. O.; Stoddart, J. F. *Org. Lett.* **2006**, *8*, 2205. This situation also arises in the trisradical complexes of $BIPY^{(\bullet+)}$⊂**CBPQT**$^{2(\bullet+)}$. See refs 25a, 25b, 25g, and 25i.

(30) Bock, C. R.; Connor, J. A.; Gutierrez, A. R.; Meyer, T. J.; Whitten, D. G.; Sullivan, B. P.; Nagle, J. K. *J. Am. Chem. Soc.* **1979**, *101*, 4815.

(31) (a) Ashton, P. R.; Ballardini, R.; Balzani, V.; Credi, A.; Ruprecht, K.; Ishow, E.; Kleverlaan, C. J.; Kocian, O.; Preece, J. A.; Spencer, N.; Stoddart, J. F.; Venturi, M.; Wenger, S. *Chem.—Eur. J.* **2000**, *6*, 3558. (b) Balzani, V.; Clemente-León, M.; Credi, A.; Ferrer, B.; Venturi, M.; Flood, A. H.; Stoddart, J. F. *Proc. Natl. Acad. Sci. U.S.A.* **2006**, *103*, 1178.

(32) Nonzero flux of this kind, under the constant application of a single stimulus, is a key feature of the motor mechanisms that drive biological motor molecules. See ref 12d.

(33) McGonigal, P. R.; Stoddart, J. F. *Nat. Chem.* **2013**, *5*, 260.

(34) Brown, C. L.; Philp, D.; Spencer, N.; Stoddart, J. F. *Isr. J. Chem.* **1992**, *32*, 61.

(35) Ashton, P. R.; Blower, M.; Philp, D.; Spencer, N.; Stoddart, J. F.; Tolley, M. S.; Ballardini, R.; Ciano, M.; Balzani, V.; Gandolfi, M. T.; Prodi, L.; McLean, C. H. *New J. Chem.* **1993**, *17*, 689.

(36) Tannor, D. J.; Marten, B.; Murphy, R.; Friesner, R. A.; Sitkoff, D.; Nicholls, A.; Ringnalda, M.; Goddard, W. A., III; Honig, B. *J. Am. Chem. Soc.* **1994**, *116*, 11875.

(37) *Jaguar*, version 7.0; Schrödinger, LLC: New York, 2007.